

Articles

Structure-Based Discovery of Nonpeptidic Small Organic Compounds To Block the T Cell Response to Myelin Basic Protein

Niklas K. U. Koehler,[†] Chao-Yie Yang,[‡] Judith Varady,[‡] Yipin Lu,[‡] Xiong-wu Wu,[‡] Ming Liu,[‡] Daxu Yin,[‡] Margreet Bartels,[†] Bi-ying Xu,[†] Peter P. Roller,[§] Ya-qiu Long,[§] Peng Li,[§] Michael Kattah,[†] Marjorie L. Cohn,^{||} Kelly Moran,[†] Eureka Tilley,[†] John R. Richert,^{*,†,⊥} and Shaomeng Wang^{*,‡}

Departments of Microbiology and Immunology, Neurology, and Pathology, Georgetown University Medical Center, Washington, D.C. 20007, Departments of Internal Medicine and Medicinal Chemistry, University of Michigan, Ann Arbor, Michigan 48109-0934, and Laboratory of Medicinal Chemistry, National Cancer Institute, National Institutes of Health, Frederick, Maryland 20892

Received July 30, 2003

We have utilized a computational structure-based approach to identify nonpeptidic small organic compounds that bind to a human leukocyte antigen (HLA) DR1301 molecule (HLA-DR1301 or DR1301) and block the presentation of myelin basic protein peptide 152–165 (MBP 152–165) to T cells. A three-dimensional (3D) structure of DR1301 was derived by homology modeling followed by extensive molecular dynamics simulation for structural refinement. Computational structure-based database searching was performed to identify nonpeptidic small-molecule candidates from the National Cancer Institute (NCI) database containing over 150 000 compounds that can effectively interact with the peptide-binding groove of the HLA molecule. By *in vitro* testing of 106 candidate small molecules, two lead compounds were confirmed to specifically block IL-2 secretion by DR1301-restricted T cells in a dose-dependent and reversible manner. The specificity of blocking DR1301-restricted MBP presentation was further validated in a binding assay using an analogue of the most potent lead compound. Computational docking was performed to predict the three-dimensional binding model of these confirmed small molecule blockers to the DR1301 molecule and to gain structural insight into their interactions. Our results suggest that computational structure-based searching is an effective approach to discover nonpeptidic small organic compounds to block the interaction between DR1301 and T cells. The nonpeptidic small organic compounds identified in this study are useful pharmacological tools to study the interactions between HLA molecules and T cells and a starting point for the development of a novel therapeutic strategy for the treatment of multiple sclerosis (MS) or other immune-related disorders.

Introduction

CD4⁺ T cells are thought to play a pivotal pathological role in mediating an autoimmune attack against myelin components in multiple sclerosis (MS).¹ It is believed that disease-associated human leukocyte antigen (HLA) molecules bind certain immunodominant peptides and that these complexes, in turn, trigger autoreactive T cell receptors (TCRs). Myelin basic protein (MBP) is one of several putative autoantigens suspected in MS. Of two regions on the MBP molecule that have been shown to be immunodominant for human T cells, MBP 152–165 is frequently restricted by DR1301 (DR α , β 1*1301),^{2,3} and epitopes within MBP 83–105 are often restricted by DR2 (DR α , β 1*1501 and DR α , β 5*0101) and some-

times by DR1301.^{4,5} These HLA types are over-represented in various populations of MS patients.^{6–8} The amino acid residues that anchor these MBP peptides to HLA-DR, and which likely interact with binding pockets in the floor of the DR antigen binding groove, have also been defined.^{9–11}

Previous attempts to interfere with MBP recognition by autoreactive T cells, targeting major histocompatibility complex (MHC) molecules, have included MHC-specific monoclonal antibodies (MAbs) and competitor peptides with high binding affinity to the MHC.^{12–14} Both approaches are less than optimal. There is the possibility of an anti-idiotypic or antipeptide immune response¹⁵ being developed. Peptides in general can be rapidly degraded *in vivo* by peptidases. Both the antibodies and peptides cannot readily penetrate through the blood–brain barrier.

On the other hand, nonpeptidic small organic molecules have several therapeutic advantages over antibodies or peptides.¹⁶ They are more resistant to enzymatic cleavage. Many small molecule drugs may enter

* Corresponding authors. E-mail: richertj@georgetown.edu (J.R.R.), shaomeng@umich.edu (S.W.).

[†] Microbiology and Immunology, Georgetown University Medical Center.

[‡] University of Michigan.

[§] National Institutes of Health.

^{||} Department of Pathology, Georgetown University Medical Center.

[⊥] Department of Neurology, Georgetown University Medical Center.

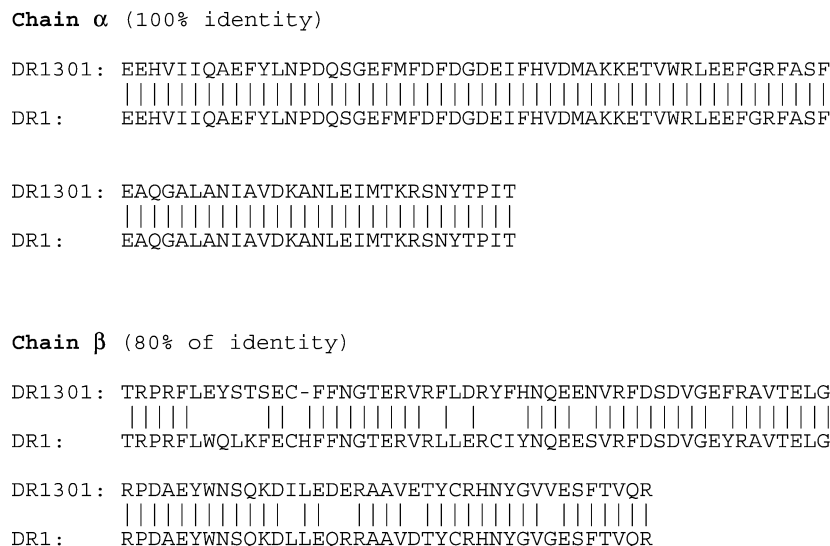


Figure 1. Alignment between DR1301 and DR1. Only residues at the binding site were included in the alignment and homology modeling (81 residues for chain α and 90 residues for chain β). There is a 100% identity for chain α between DR1301 and DR1 (residues 3–83 of chain α in the X-ray structure of DR1). There is 80% of identity for chain β between DR1301 and DR1 (residues 3–93 of chain β in the X-ray structure of DR1).

immune-privileged organs, e.g., crossing the blood–brain barrier, and can be absorbed if given orally. In addition, nonpeptidic small organic molecules are unlikely to elicit unintended T cell activation.

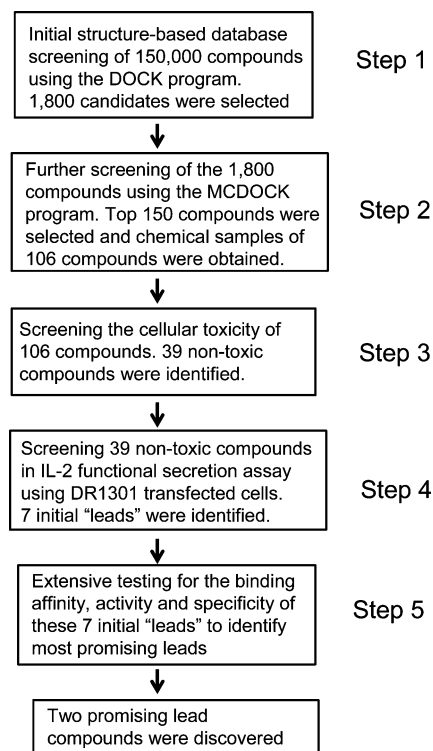
In this paper, we have used a computational structure-based database search to identify small molecule candidates from 150 000 compounds in the National Cancer Institute (NCI) three-dimensional (3D) database that can effectively interact with DR1301 molecules by computational docking and scoring. The selected small molecule candidates were tested *in vitro* for their ability to block MBP 152–165 peptide presentation by DR1301. We also addressed the specificity of the molecules for blocking DR1301 versus another closely related HLA molecule (HLA-DR1501). Finally, we employed computational docking to gain structural insight into the binding of the most potent lead compound and two of its analogues. The overall procedures used in our studies are summarized in Chart 1.

Results

The Modeled Structure of DR1301. The computer program MODELLER as implemented into the InsightII program¹⁷ was used to model the 3D structure of the DR1301 molecule by homology modeling based on the crystallized structure of DR1 in complex with influenza hemagglutinin peptide 306–318¹⁸ as the template structure. DR1301 has a high sequence homology with DR1, with 100% identity between their α chains and 80% identity between their β chains. The sequence alignment between DR1301 and DR1 is provided in Figure 1. Because of the high sequence identity between these two proteins, the 3D structure of DR1301 can be modeled accurately using the high-resolution X-ray structure of DR1 as the template structure.

We have previously shown that MBP 152–165 interacts with DR1301 molecule.⁹ The MBP 152–165 peptide has an amino acid sequence of K(152)IFKLGGRDSRSGS. Using Ala-substituted MBP peptides, we deduced that three residues in the MBP 152–165 peptide, i.e., F154, R159, and R162, are predominantly responsible for the

Chart 1. Stepwise Computational and Experimental Procedures for the Discovery of Small Molecule Nonpeptidic Ligands for DR1301



interactions between the MBP peptide and DR1301 molecule.⁹ This information was thus used to assist the modeling of the structure of MBP 152–165 in complex with DR1301. In the modeled complex structure, the peptide backbone atoms of MBP 152–165 peptide were overlaid with the peptide backbone atoms of the influenza hemagglutinin peptide 306–318 in the template structure, and the F154 side chain occupies a hydrophobic pocket in DR1301, while R159 and R162 occupy a very large negatively charged pocket in DR1301. The obtained complex was energy-minimized using the CHARMM program. Extensive molecular dynamics

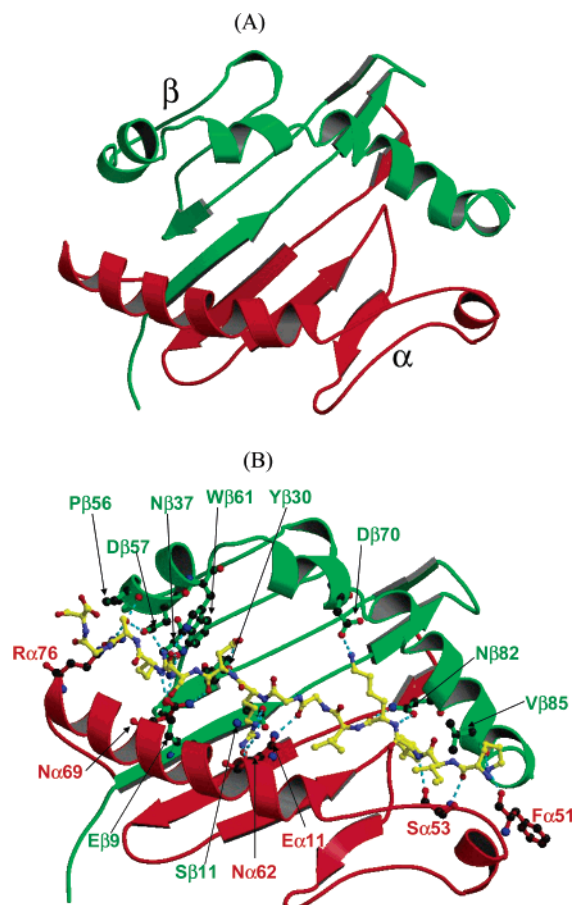


Figure 2. Modeled DR1301 3D structure and its binding groove. Part A depicts the backbone topology of the modeled DR1301 three-dimensional structure. Its α and β chains are colored red and green, respectively. Part B shows the hydrogen-bond interaction between the MBP 152–165 peptide and the modeled DR1301. The carbon atoms and bonds in the peptide are colored yellow, and the oxygen and nitrogen atoms are colored red and blue. Residues from DR1301 colored green and red are in α and β chains, respectively. All oxygen atoms are colored red and nitrogen atoms blue. Carbon atoms in DR1301 are colored black. Distances of the hydrogen bonds between the peptide and DR1301 in Å calculated by the Ligplot⁴⁰ program are F α 11 (2.86, 2.69), F α 51 (2.69), S α 53 (3.34, 2.94), N α 62 (2.99), N α 69 (3.24, 2.98), R α 76 (2.67, 3.01) and E β 9 (2.65), S β 11 (2.60, 2.92), Y β 30 (2.86, 2.94), N β 30 (2.61, 2.75), P β 56 (2.54), D β 57 (2.70, 2.65), W β 61 (2.91), D β 70 (2.50), N β 82 (2.90, 2.97), V β 85 (2.59), respectively.

(MD) simulation has been often used to refine the modeled structures obtained from homology modeling for improving modeling accuracy.³⁷ Thus, the modeled DR1301 structure was refined through extensive MD simulation in explicit water. The obtained HLA DR1301 3D complex structure was used for structure-based database screening with the peptide MBP 152–165 being deleted from the structure (Figure 2).

Structure-Based Database Screening for Compounds Predicted To Bind DR1301. We searched a subset of the NCI chemical database, consisting of 150 000 nonpeptidic, synthetic compounds and natural products, whose chemical samples were available with sufficient quantity for experimental testing. The DOCK program was used to perform the computational structure-based database screening. The grid box was defined to cover the entire binding pocket in the DR1301 structure where the MBP peptide binds. Default pa-

rameters in the DOCK program were used. The top 1800 compounds from the 150 000 compounds with the best DOCK scores were selected for more detailed computational docking refinement and scoring using the MCDOCK program.²⁰ The top 150 compounds were considered as potential DR1301 ligands. Chemical samples of 106 compounds out of these 150 candidate compounds were obtained from the NCI and tested for their ability to block antigen presentation by DR1301, as described below.

Biological Evaluation of the Activity and Specificity of Potential Small Molecule Inhibitors To Block Antigen Presentation by DR1301. Our objective was to identify nontoxic compounds that were capable of blocking MBP presentation by DR1301. For this purpose, the toxicity of the 106 candidate compounds was evaluated by trypan blue staining of the TCR and HLA transfectants after culture with a high concentration (500 μ M) of each compound. Thirty-nine compounds out of 106 were found not to significantly alter cell viability and were considered as nontoxic and they were further tested for their ability to block DR1301 in *in vitro* assays.

As previously shown, DR1301-restricted TCR transfectants are readily stimulated with MBP peptide 152–165, as measured by IL-2 secretion.⁹ Initially, we tested the potency of the 39 nontoxic compounds to block IL-2 secretion by DR1301-restricted TCR-transfected cells in the presence of 100 μ g/mL (67 μ M) of MBP peptide 152–165. Of the 39 nontoxic compounds, seven blocked IL-2 secretion in a dose-dependent manner. However, three of the seven compounds inhibited IL-2 secretion at 125 μ M by less than 33% and were considered as weak inhibitors and not further pursued. Of the remaining four compounds, one strongly inhibited IL-2 secretion of DR1501-restricted TCR transfected cells in the presence of MBP 83–97, suggesting a nonspecific inhibition of both DR1301 and DR1501 molecules. A second compound did not show sufficient reversal of IL-2 secretion at higher doses of MBP 152–165 in a subsequent experiment and also inhibited proliferation of the transfectants alone as measured by [³H]thymidine incorporation (data not shown), suggesting nonspecific toxicity to cells. Both compounds were therefore excluded from further consideration.

The two remaining compounds, **1** (NSC 687766) and **2** (NSC45598), potently blocked IL-2 secretion (Figure 3) and were considered as promising lead compounds. Lead compound **1** displayed a higher potency than lead compound **2** (Figure 3). The chemical structures of these two lead compounds are provided in Chart 2.

Next, we evaluated the ability of the two lead compounds to block IL-2 secretion by DR1301-restricted TCR transfected cells in the presence of different concentrations of MBP peptide 152–165. The inhibition of IL-2 secretion by these two lead compounds was reversed by higher doses of MBP peptide 152–165 (Figure 4), suggesting that the inhibition of IL-2 secretion by these lead compounds was indeed due to their blocking of presentation of MBP peptide 152–165 to the DR1301-restricted TCR. Even at the high MBP concentration of 1200 μ g/mL (800 μ M), the lead compound **1** was able to inhibit IL-2 secretion by 17.2%. In contrast, inhibition of IL-2 secretion by lead compound **2** was

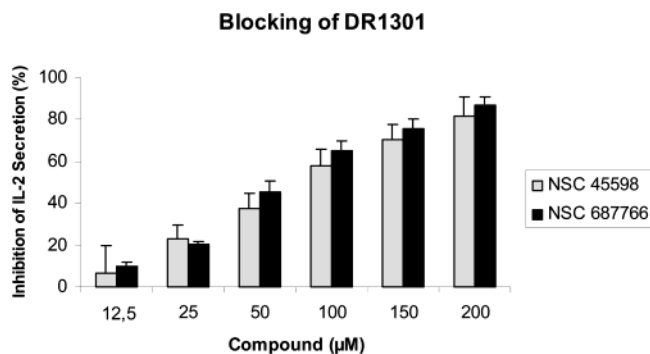


Figure 3. Blocking of DR1301 by lead compound **1** (NSC 687766) and **2** (NSC 45598), expressed as inhibition of IL-2 secretion by DR 1301-restricted TCR transfectants. TCR transfectants were stimulated with 100 μg/mL MBP 152–165 presented by DR1301 transfectants as described in Methods. Results are presented as mean percent inhibition with standard deviations.

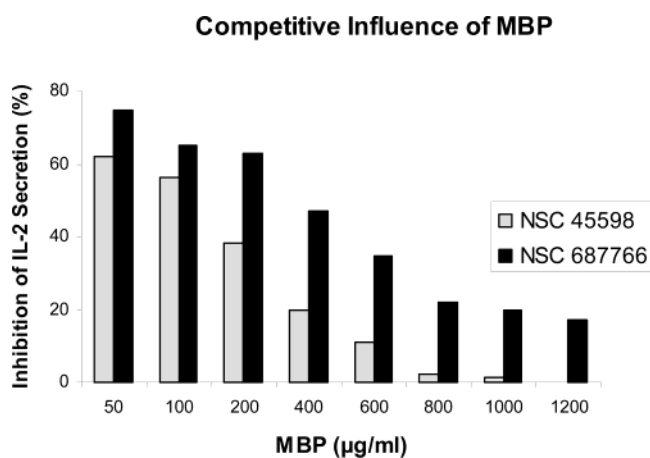
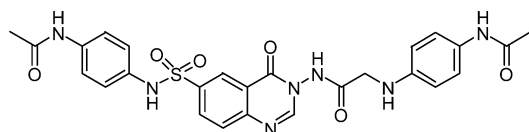
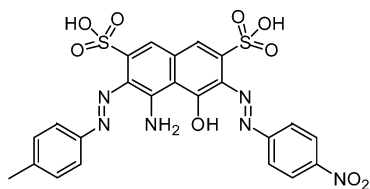


Figure 4. Competitive influence of increasing concentrations of MBP 152–165 at a fixed concentration (100 μM) of the DR1301 blocking lead compounds **1** (NSC 687766) and **2** (NSC 45598). Reversal of DR1301 blockade is expressed as decreasing inhibition of IL-2 secretion by DR1301-restricted TCR transfectants with increasing concentrations of MBP.

Chart 2. Chemical Structures of Lead Compound **1** (NSC 687766) and Lead Compound **2** (NSC 45598)



1 (NSC 687766)



2 (NSC 45598)

almost completely reversed by an MBP concentration of 800 μg/mL (533 μM), again indicating a higher potency of compound **1**.

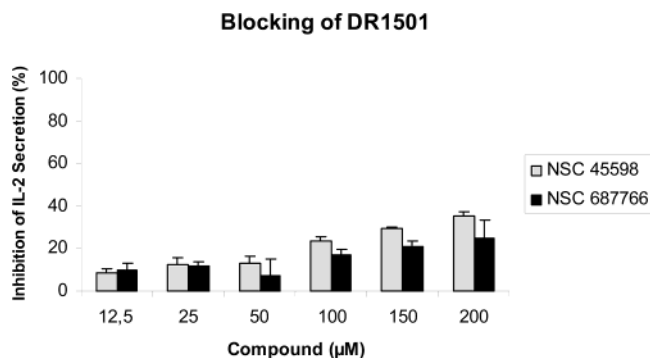
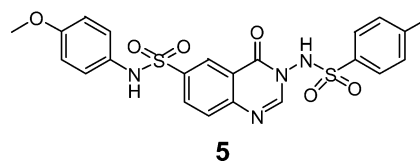
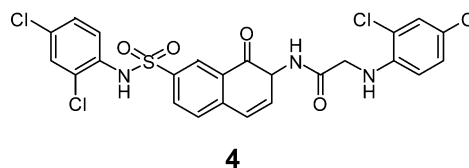
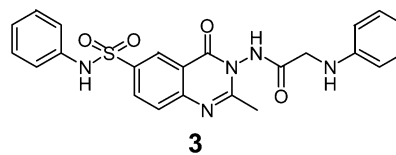


Figure 5. Test for specificity of lead compound **1** (NSC 687766) and **2** (NSC 45598) by measuring inhibition of IL-2 secretion by DR1501-restricted TCR transfectants at different concentrations of the compounds. TCR transfectants were stimulated with 100 μg/mL MBP 83–97 in the presence of DR1501 transfectants as described in Methods. Results are presented as mean percent inhibition with standard deviations.

Chart 3. Chemical Structures of the Three New Analogues of Lead Compound **1**



It was previously shown that MBP peptide 83–97 stimulated IL-2 secretion in HLA-DR1501-restricted TCR transfected cells. To evaluate the specificity of the two lead compounds, we tested their ability to block IL-2 secretion by DR1501-restricted TCR transfected cells in the presence of 100 μg/mL (67 μM) MBP peptide 83–97. As illustrated in Figure 5, compound **1** showed the highest degree of specificity for inhibiting antigen presentation by DR1301 as opposed to presentation of MBP 83–97 by DR1501, indicating that compound **1** represents a selective inhibitor for DR1301 versus its closely homologous DR1501 molecule.

To gain an understanding of the preliminary structure–activity relationship of compound **1**, we searched the NCI database to identify its analogues. Three structurally closely related new analogues were identified (**3–5**) and their chemical structures are shown in Chart 3. Of note, these three analogues received lower scores in the DOCK screening and were ranked below the top 1800 compounds. Close examination showed that the docked structures for these analogues as predicted by the DOCK program were somewhat different from

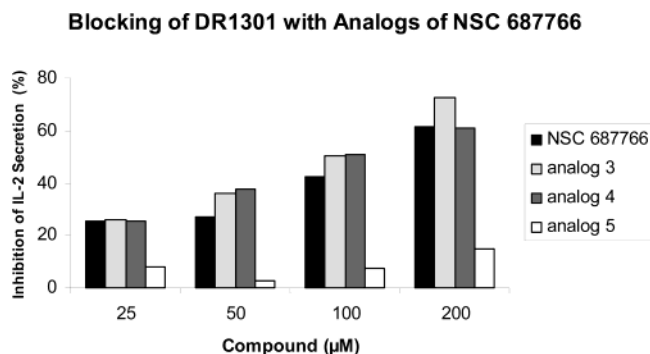


Figure 6. Blocking of DR1301 by three structurally closely related analogues of lead compound **1** (NSC 687766) expressed as inhibition of IL-2 secretion by DR1301-restricted TCR transfectants at different concentrations of the compounds. TCR transfectants were stimulated with 100 $\mu\text{g}/\text{mL}$ MBP 152–165 and DR1301 transfectants. In contrast to analogue **5**, analogues **3** and **4** blocked DR1301 to a degree similar to that of the lead compound.

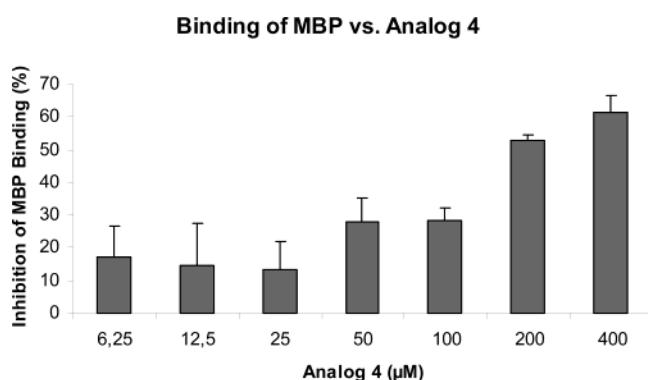


Figure 7. Competitive binding assay using DR1301 transfectants, 200 μM biotinylated MBP 152–165, and increasing concentrations of analogue **4** (described in Methods). Analogue **4** reversed the binding of MBP from DR1301 molecules in a dose-dependent manner, indicating the specific interaction of the compound with DR1301. Results are presented as mean percent inhibition with standard deviations.

that of the lead compound **1**, probably due to the short docking time used in the computational structure-based screening.

These analogues were tested for their inhibitory activity on IL-2 secretion by the DR1301-restricted TCR transfectants and for their specificity by using the DR1501-restricted TCR transfectants. The new analogues **3** and **4** have a potency similar to that of compound **1** (Figure 6). In comparison, analogue **5** has a diminished activity in inhibiting IL-2 secretion by DR1301-restricted TCR transfectants. In this assay, all compounds exhibited very low levels of DR1501 inhibition (less than 1%).

To further test whether the inhibition of antigen presentation by these small molecule inhibitors was due to their binding of DR1301, we used a direct competitive in vitro binding assay (see Methods for details). In this assay, we tested the ability of these compounds to compete off the biotinylated MBP 152–165 peptide from the DR1301 molecules. Inhibition of MBP binding by analogue **4** is shown in Figure 7. Analogue **4** competed off the binding of biotinylated MBP 152–165 peptide (200 $\mu\text{g}/\text{mL}$ or 133 μM) to DR1301 in a dose-dependent manner with an IC_{50} value of 200 μM , suggesting that analogue **4** has a binding affinity to DR1301 molecule

approximately 2 times less than the MBP 152–165 peptide in this direct competitive binding assay.

Finally, we evaluated the influence of analogues **3–5** on proliferation of the transfectants alone by culturing the compounds with each cell line and measuring [^3H] thymidine incorporation. As expected, we did not observe any inhibitory effects of the compounds on proliferation (data not shown), confirming that these compounds are not generally toxic to cells.

Structural Basis of the Binding of Nonpeptidic, Small Molecule Inhibitors to DR1301. To understand the structural basis of the binding of these nonpeptidic, small molecule ligands to DR1301, we performed computational docking studies of lead compound **1** and its analogues **4** and **5** using the GOLD docking program.³⁹ GOLD was employed in this study because of its high accuracy in reproducing experimentally determined binding models of ligands to their protein targets based upon our recent study.⁴⁰ Ligplot⁴¹ was used to analyze the hydrogen bonding and hydrophobic interaction between DR1301 and ligands based upon the predicted binding models by the GOLD program.

The predicted binding model for lead compound **1** in complex with DR1301 is depicted in Figure 8A. Analysis of this binding model showed that the right phenyl ring in lead compound **1** inserts into the hydrophobic pocket primarily formed by two phenylalanine residues from the α chain (F α 24 and F α 54) and one phenylalanine residue from the β chain (Y β 78) and occupied by leucine 156 (L156) of MBP peptide. The left phenyl ring in **1** is in close contact with phenylalanine 30 and tryptophan 61 from the β chain (Y β 30 and W β 61). In addition, a number of hydrogen bonds were formed between lead compound **1** and DR1301. However, the number of hydrogen bonds formed between lead compound **1** and DR1301 were fewer than those formed between MBP peptide and DR1301 (Figure 2B). Furthermore, the hydrophobic pocket in DR1301 occupied by phenylalanine residue 154 was not occupied by lead compound **1**.

The predicted binding model of analogue **4** is shown in Figure 8B. Overall, compound **4** has a similar binding model as lead compound **1**. The noticeable difference is that the left phenyl ring in **4** is in close contact with phenylalanine 47 and 67 residues from the β chain (F β 47 and I β 67) and the hydrogen-bonding network is also different from that for lead compound **1**.

The predicted binding model of the inactive analogue **5** is shown in Figure 8C. Overall, compound **5** adopts a similar binding model as lead compound **1** and analogue **4**. The most significant difference is the interaction between its right phenyl ring and DR1301. In both **1** and **4**, the right phenyl ring occupies the hydrophobic pocket formed by F α 24, F α 54, and Y β 78 in DR1301. In the binding model for **5**, its right phenyl ring does not insert into this hydrophobic pocket. The lack of this favorable hydrophobic interaction may explain the weaker activity of **5** than that of **1** and **4**. Taken together, our computational docking studies provide structural insights for the binding of these ligands to DR1301 and importantly a starting point for optimization to further improve their binding affinity to DR1301.

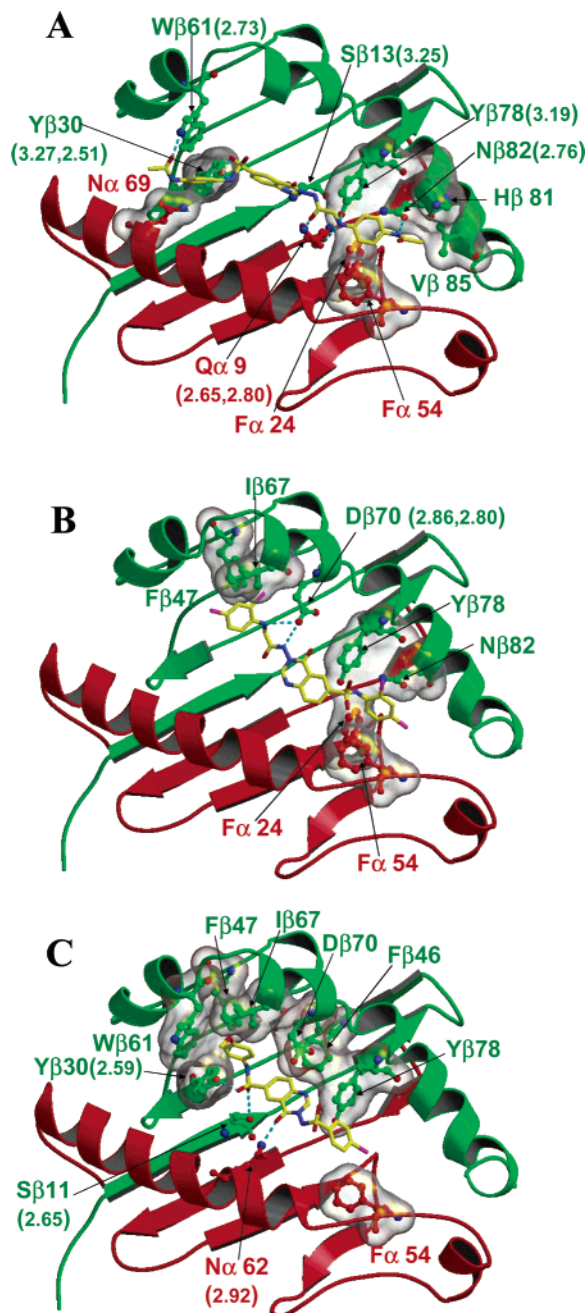


Figure 8. Predicted binding modes of lead compound **1** (NSC 687766) and its analogues **4** and **5** in the DR1301 binding pocket. DR1301 is shown as transparent for clarity. Residues of DR1301 that form van der Waals contacts with the MBP peptide are drawn in green (β chain) and red (α chain) and the molecular surface of these residues are shown as transparent. For residues of DR1301 forming hydrogen bonds with the peptide, the ball-and-stick model is used. Similar to Figure 2B, residues labeled with green and red refer to the β and α chains, respectively. Atoms are colored by atom type, except that carbon atoms of NSC 687766 (Figure 8A), analogue **4** (Figure 8B), and analogue **5** (Figure 8C) are colored yellow. The interaction between DR1301 and each ligand is discussed in text. Numbers in parentheses are distances of the hydrogen bonds in Å between ligands and DR1301 calculated by the Ligplot⁴⁰ program.

Discussion

A number of human inflammatory and autoimmune diseases have well-documented associations with particular HLA types. That is, particular HLA types are

over-represented among the patient population in question.^{6–8} The assumption is that the pathogenesis of the disease is in some way related to the presentation of an autoantigen and/or an antigen of infectious origin to disease-causing T cells by the designated HLA molecule. Thus, targeting the relevant HLA molecule as a means of blocking the pathologic immune response represents a potentially attractive approach to therapy. As the relevant autoantigen has only rarely been identified for a given autoimmune disease (e.g., the nicotinic acetylcholine receptor in myasthenia gravis), targeting a specific antigen or T cell receptor for other autoimmune diseases involves considerable speculation as to what should be the relevant target. Because there is considerable redundancy among HLA molecules in their ability to present antigens of infectious origin to the immune system, blocking one such molecule that has disease relevance for an autoimmune process is not likely to have significant adverse consequences with regard to susceptibility to infectious diseases. Indeed, blocking murine MHC molecules in vivo by using either MHC-specific MAbs¹² or MHC-binding peptides^{13,14} has been of considerable benefit and well-tolerated in animal models. However, in a recently completed phase II human clinical trial of an altered MBP 83–99 peptide ligand (CGP77116) in multiple sclerosis, CGP77116 was very immunogenic in vivo and resulted in substantial expansion of T cells specific for this altered peptide ligand that were cross-reactive with the native autoantigen and de novo-activated T cells specific for this altered peptide ligand often expressed a proinflammatory phenotype.¹⁵

Nonpeptidic small organic molecules may have several advantages over either MAbs or HLA-blocking molecules of peptide origin. Nonpeptidic small molecules are more resistant to enzymatic cleavage than peptide-based ligands, may be orally available, may enter immune-privileged organs more easily, are less likely to be immunogenic themselves, and are unlikely to elicit unintended T cell activation. The latter property is in contrast to altered peptide ligands,¹⁵ which depend on the juxtaposition of an antigen-presenting cell and T cell in order to suppress the immune response in question.

Our present study explores a novel strategy using nonpeptidic, small organic compounds to block the presentation of MBP peptide to T cell receptors. Using a computational structure-based search of 150 000 synthetic compounds and natural products, with subsequent in vitro validation using functional and binding assays, we discovered and confirmed two nonpeptidic small organic molecules that are capable of binding to the DR1301 molecule and thereby blocking presentation of MBP 152–165 to the T-cell receptor. We further demonstrated that lead compound **1** and two analogues, **3** and **4**, display specificity for blocking DR1301 versus another closely related HLA-DR1501 molecule in functional assays. The potency of lead compound **1** is similar to that of the MBP peptide in both functional and binding assays. Our computational modeling studies shed light on the structural binding of these small molecule inhibitors to DR1301. Although the potency and specificity of these small molecules may need to be further improved for therapeutic use, our study provides the proof-of-concept for this novel approach and suggests

that further exploration of this approach would be warranted.

Methods

Cell Lines. The murine T cell hybridoma cell line BW58 $\alpha^{-}\beta^{-}$ transfected with human TCR α and β cDNAs was used as previously described.⁹ The original untransfected line had been a kind gift of B. Malissen and W. Born. The DR1301-restricted TCR cDNA was originally cloned from a human T cell clone specific for MBP peptide 152–165.^{2,9} The DR1501-restricted TCR cDNA was the kind gift of D. Hafler and was originally cloned from a T cell clone specific for MBP peptide 83–97.²⁶ The parental DAP.3 murine fibroblast cell line transfected with DR(α , β 1*1301) or DR (α , β 1*1501) were the kind gifts of C. Hurley and S. Rosen-Bronson, respectively.^{27,28} All cell lines were maintained in DMEM supplemented with 10% fetal calf serum, 50 U/mL penicillin G, 50 mg/mL streptomycin, 1 mM sodium pyruvate, 2 mM glutamine, and 10 mM HEPES buffer (all Gibco/BRL, Gaithersburg, MD). TCR- and HLA-transfectants were expanded in the presence of 1 mg/mL G418 (Gibco/BRL), or 1 mg/mL G418 and 1 mg/mL hygromycin (Calbiochem, San Diego, CA), respectively.

Cytofluorometric Analysis. Expression of murine CD3 ϵ and human V β 22 on transfected BW58 $\alpha^{-}\beta^{-}$ cells and HLA-DR on transfected Dap.3 cells was monitored by flow cytometry (FACStar^{Plus}, Becton-Dickinson, Mountainview, CA) using PE-labeled MAbs to murine CD3 ϵ (Gibco/BRL), unlabeled mouse anti-human TCR V β 22 (Immunotech, Westbrook, ME) with PE-labeled secondary goat F(ab')₂ specific for mouse IgG (Gibco/BRL), and FITC-labeled anti-HLA-DR (Becton-Dickinson, Mountainview, CA), respectively. Labeled isotype-matched control Abs were used to exclude nonspecific binding.

Functional Activation and Blocking Assays. Cells were washed and resuspended in DMEM complete medium without antibiotics. A total of 10⁵ TCR-transfected or untransfected (control) BW58 $\alpha^{-}\beta^{-}$ cells and an equal number of DR-transfected or untransfected (control) Dap.3 cells were incubated with MBP 152–165 or MBP 83–97 and various concentrations of small organic compounds, using U-bottom 96-well plates (Costar). Cell culture supernatants were harvested after 2 days and stored at –70 °C until use. IL-2 cytokine concentrations (pg/mL) in the supernatants were measured by ELISA (Genzyme, Cambridge, MA) according to the manufacturer's instructions. Multiple measurements of the same sample for an individual data point showed <10% variation. Inhibition of IL-2 secretion by individual compounds was calculated using the following formula:

$$\% \text{ inhibition} = \left(1 - \frac{\text{IL-2 concentration with compound}}{\text{IL-2 concentration without compound}} \right) \times 100\%$$

Competitive Binding Assays. Peptide binding assays were performed using an adaptation of methods previously described.^{32,33} For each measurement, 1.5 \times 10⁶ DR1301-transfected DAP.3 cells were used. After washing two times with Hank's balanced salt solution (HBSS), the cells were fixed with 1% paraformaldehyde PBS for 10 min. After washing with RPMI medium and then with PBS, the cells were resuspended in 200 μ L binding buffer consisting of 150 mM citrate-phosphate buffer, pH 4.4, 5 mM EDTA, 1 mM iodoacetamide, 1 mM benzamidine, and 1 mM Pefabloc. Biotinylated MBP peptide was added at 200 μ g/mL (MBP 152–165). BSA was added at 1%. Small organic compounds were added at concentrations ranging from 6.25 to 400 μ M and incubated overnight in a shaking waterbath at 37 °C, after which they were washed and lysed with 100 μ L lysis buffer consisting of 50 mM Tris, pH 7.5, 1% Nonidet-P40, 0.15 M NaCl, 5 mM EDTA, 1 mM Pefabloc, 10 μ g/mL leupeptin, and 10 μ g/mL pepstatin for 40 min. After centrifuging for 10 min in a refrigerated microcentrifuge, 100 μ L of supernatant containing the cell membrane fragments was transferred to each well of a 96-well plate precoated with L234 (anti-DR) antibody to which had been added 100 μ L of 0.75% *n*-octyl- β -D-glucopy-

ranoside (Sigma) (pH 8.0) to neutralize the lysis buffer. The plate was incubated overnight at 4 °C. After washing five times with 400 μ L PBS/0.05% Tween 20, the wells were incubated with streptavidin-peroxidase for 1 h at room temperature. Substrate was added, followed 10 min later by stop solution. OD was measured at 450 nm in an ELISA reader. Competition was calculated using the following formula:

$$\% \text{ inhibition} = \left(1 - \frac{\text{OD}_{\text{with compound}} - \text{OD}_{\text{background}}}{\text{OD}_{\text{without compound}} - \text{OD}_{\text{background}}} \right) \times 100\%$$

Molecular Modeling of the DR1301 Structure in Complex with MBP 152–165 Peptide. The DR1301 model in complex with MBP 152–165 peptide was built using homology modeling based on the crystal structure of HLA-DR1 in complex with influenza hemagglutinin 306–318 (pdb code 1DLH).¹⁸ The MBP 152–165 peptide was modeled based on the peptide in the template (influenza hemagglutinin 306–318) to allow MBP side chains F154, R159, and R162 to form favorable interactions with the HLA molecule. We have previously shown that these MBP residues are involved in interactions with DR1301.⁹ The orientations of several side chains around these three peptide residues were chosen from the rotamer library of the InsightII program package³⁰ to optimize HLA-peptide interactions.

Energy Minimization of the Complex Was Performed Using the CHARMM Program. Quanta program²⁹ took three steps: first, 500 steps of steepest descent minimization steps with all backbone atoms fixed; second, 500 steps of adopted-basis Newton Raphson (ABNR) minimization cycles with trace atoms fixed; and finally, 5000 steps of ABNR cycles without any restraints.

The minimized complex structures were then subjected to structural refinement using molecular dynamics simulation method using the Amber program (version 7).³⁴ The whole complex system was embedded in the explicit water with a cubic box size of 10 Å in each dimension. The TIP3P water model³⁵ was used. The MD simulation was started with 500 steps of energy minimization followed by 40 ps of equilibration where the temperature of the system was slowly raised to 298 K. A 500 ps run of the equilibrated system was then performed. All the MD simulations were NTP simulation ($T = 298$ K and $P = 1$ atm). The SHAKE algorithm was used to fix the bonds involving hydrogen and the particle mesh Ewald summation method³⁶ was used for long-range electrostatic interactions. The nonbonded cutoff distance was set at 10 Å. The time step was 2 fs, and the neighboring pairs list was updated in every 20 steps. In the MD simulation, the backbone atoms of the DR1301 molecule were constrained by a weak harmonic force with the force constant being 10 kcal/mol Å² with reference to the initial minimized structure.

Computational Structure-Based Database Searching. The refined structure of DR1301 was used for structure-based database searching of the NCI 3D database.²¹ Although the current version of the NCI database contains more than 250 000 publicly accessible compounds,²² our search was performed on a subset of the NCI database for which a chemical sample was available with sufficient quantity for biological testing (approximately 150 000 compounds). The 3D coordinates of these 150 000 compounds were generated using the CONCORD program, described previously.²² For compounds with chiral centers, if the chiral center information was recorded in the original NCI database, the information was used to generate the correct chiral center. If such information was not recorded due to historical reasons, the chiral center was then randomly assigned during the generation of the 3D coordinates. It was one of the major drawbacks for some of the compounds in the NCI 3D-database.

The program DOCK (version 4.0.1) was employed.¹⁹ All residues within 5 Å from the MBP 152–165 peptide in the DR1301 complex structure were included in the binding site used for screening. United atom KOLLMAN charges were assigned for the protein using the BIOPOLYMER menu in the

Sybyl program.²³ Because of its general applicability, the Geisterger method, as implemented in Sybyl, was used to assign charges to the NCI compounds. The protonation state of the compounds (formal charges) was assigned according to the expected value at the physiological pH of 7.4.

The interactions between the MBP peptide and DR1301 in the modeled complex structures define the crucial binding elements between them. Thus, the spheres used in the DOCK program were defined in part by the coordinates of the MBP peptide in the modeled complex structure with DR1301. The conformational flexibility of the compounds from the database was considered, and their positions and conformations were optimized using single anchor search and torsion minimization. Fifty configurations per ligand building cycle and 100 maximum anchor orientations were used in the anchor-first docking algorithm. All docked configurations were energy minimized using 10 iterations and two minimization cycles. A scaling factor of 0.5 was used for the electrostatic interaction calculations. The sum of the electrostatic and van der Waals interactions as calculated in the DOCK program was used as the ranking score. The top-scoring 1800 compounds with a minimal docking score of -40 kcal/mol were selected as potential inhibitors for DR1301, which were further screened using the MCDOCK program.²⁰

For computational database screening of a large chemical database (150 000 compounds in our case) using the DOCK program, the computing time spent on each small molecule was very limited (typically within a few seconds). The very short computing time spent on each small molecule limited the accuracy for binding model prediction. For this reason, we employed the MCDOCK program,²⁰ recently developed in our laboratory, to perform more detailed computational docking studies for those 1800 top-ranked compounds selected from the DOCK results to DR1301. A total of 1 000 000 simulation steps were used for each ligand. The calculated interaction energy between a small molecule and DR1301 based on the final predicted docked structure was used as the docking score for ranking these 1800 compounds. Chemical samples of the top-ranked 150 compounds, which had minimal interaction energy of -60 kcal/mol, were requested from the NCI, and samples of 106 compounds were available for biological testing.

Computational Docking Studies. The initial 3D structures of the lead compound and its analogues were built and minimized using the SYBYL program (version 6.9.1)³⁸ and Tripos force field parameters. Compound **1** and its analogues were then docked into the binding site of the refined DR1301 structure using Gold 2.0.³⁹ The radius of the binding site was defined as 16 Å, which was sufficiently large enough to encompass all possible docked modes for ligands. For each genetic algorithm (GA) run, a maximum number of 100 000 operations were performed on a population of five islands of 100 individuals. Operator weights for crossover, mutation, and migration were set to 95, 95, and 10, respectively. The docking was terminated after 20 runs for each ligand. GoldScore and ChemScore implemented in Gold (version 2.0) were used separately as the fitness function to evaluate the docked conformations. Twenty highest ranked conformations for each fitness function were saved for docking modes analysis. The highest ranked docked conformations of lead compound **1** and its two analogues **4** and **5** using ChemScore are provided in Figure 8.

Acknowledgment. The authors thank Dr. Karen Cresswell for performing the cytofluorographic analyses. This work was supported by National Multiple Sclerosis Society grants PP0575 and RG2943A7/1, the Lombardi Cancer Center Flow Cytometry and Macromolecular Sequencing and Synthesis Shared Resource Facilities (USPHS Grant P30-CA-51008), and the Smith, Wadsworth, and Vorhees Funds. N.K.U.K. was a postdoctoral fellow of the Deutsche Forschungsgemeinschaft (KO 1719/1-1). The chemical samples used in our biological evaluations were provided by the Drug Syn-

thesis & Chemistry Branch, Developmental Therapeutics Program, Division of Cancer Treatment and Diagnosis, National Cancer Institute, National Institutes of Health, and their help on this project is highly appreciated.

References

- (1) Martin, R.; McFarland, H. F.; McFarlin, D. E. Immunological aspects of demyelinating diseases. *Annu. Rev. Immunol.* **1992**, *10*, 153–187.
- (2) Richert, J. R.; Robinson, E. D.; Johnson, A. H.; Bergman, C. A.; Dragovic, L. J.; Reinsmoen, N. L.; Hurley, C. K. Heterogeneity of the T cell receptor β gene rearrangements generated in myelin basic protein-specific T cell clones isolated from a patient with multiple sclerosis. *Ann. Neurol.* **1991**, *29*, 299–306.
- (3) Martin, R.; Jaraquemada, D.; Flerlage, M.; Richert, J.; Whitaker, J.; Long, E. O.; McFarlin, D. E.; McFarland, H. F. Fine specificity and HLA restriction of myelin basic protein-specific cytotoxic T cell lines from multiple sclerosis patients and healthy individuals. *J. Immunol.* **1990**, *145*, 540–548.
- (4) Vergelli, M.; Kalbus, M.; Rojo, S. C.; Hemmer, B.; Kalbacher, H.; Tranquill, L.; Beck, H.; McFarland, H. F.; De Mars, R.; Long, E. O.; Martin, R. T cell response to myelin basic protein in the context of the multiple sclerosis-associated HLA-DR15 haplotype: Peptide binding, immunodominance and effector functions of T cells. *J. Neuroimmunol.* **1997**, *77*, 195–203.
- (5) Martin, R.; Howell, M. D.; Jaraquemada, D.; Flerlage, M.; Richert, J.; Brostoff, S.; Long, E. O.; McFarlin, D. E.; McFarland, H. F. A myelin basic protein peptide is recognized by cytotoxic T cells in the context of four HLA-DR types associated with multiple sclerosis. *J. Exp. Med.* **1991**, *173*, 19–24.
- (6) Jersild, C.; Fog, T.; Hansen, G. S.; Thomsen, M.; Svejgaard, A.; Dupont, B. Histocompatibility determinants in multiple sclerosis, with special reference to clinical course. *Lancet* **1973**, *2*, 1221–1225.
- (7) Gorodezky, C.; Najera, R.; Rangel, B. E.; Castro, L. E.; Flores, J.; Velazquez, G.; Granados, J.; Sotelo, J. Immunogenetic profile of multiple sclerosis in Mexicans. *Hum. Immunol.* **1986**, *16*, 364–374.
- (8) Naito, S.; Kuroiwa, Y.; Itoyama, T.; Tsubaki, T.; Horikawa, A.; Sasazuki, T.; Noguchi, S.; Ohtsuki, S.; Tokuomi, H.; Miyatake, T.; Takahata, N.; Kawanami, S. HLA and Japanese multiple sclerosis. *Tissue Antigens* **1978**, *12*, 19–24.
- (9) Hastings, A. E.; Hurley, C. K.; Robinson, E. D.; Salerno, K.; Hernandez, E.; Richert, J. R. Molecular interactions between transfected human TCR, immunodominant myelin basic protein peptide 152–165, and HLA-DR13. *J. Immunol.* **1996**, *157*, 3460–3471.
- (10) Wucherpfennig, K. W.; Sette, A.; Southwood, S.; Oseroff, C.; Matsui, M.; Strominger, J. L.; Hafler, D. A. Structural requirements for binding of an immunodominant myelin basic protein peptide to DR2 isotypes and for its recognition by human T cell clones. *J. Exp. Med.* **1994**, *179*, 279–290.
- (11) Vogt, A. B.; Kropshofer, H.; Kalbacher, H.; Kalbus, M.; Rammensee, H. G.; Coligan, J. E.; Martin, R. Ligand motifs of HLA-DRB5*0101 and DRB1*1501 molecules delineated from self-peptides. *J. Immunol.* **1994**, *153*, 1665–1673.
- (12) Steinman, L.; Rosenbaum, J. T.; Sriram, S.; McDevitt, H. O. In vivo effects of antibodies to immune response gene products: Prevention of experimental allergic encephalomyelitis. *Proc. Natl. Acad. Sci. U.S.A.* **1981**, *78*, 7111–7114.
- (13) Gautam, A. M.; Pearson, C. I.; Sinha, A. A.; Smilek, D. E.; Steinman, L.; McDevitt, H. O. Inhibition of experimental autoimmune encephalomyelitis by a nonimmunogenic nonself-peptide that binds to I–Au. *J. Immunol.* **1992**, *148*, 3049–3054.
- (14) Wraith, D. C.; Smilek, D. E.; Webb, S. MHC-binding peptides for immunotherapy of experimental autoimmune disease. *J. Autoimmunity* **1992**, *5 Suppl A*, 103–110.
- (15) Bielekova, B.; Goodwin, B.; Richert, N.; Cortese, I.; Kondo, T.; Afshar, G.; Gran, B.; Eaton, J.; Antel, J.; Frank, J. A.; McFarland, H. F.; Martin, R. Encephalitogenic potential of the myelin basic protein peptide (amino acids 83–99) in multiple sclerosis: Results of a phase II clinical trial with an altered peptide ligand. *Nat. Med.* **2000**, *6*, 1167–75.
- (16) Betancur, C.; Azzi, M.; Rostene, W. Nonpeptide antagonists of neuropeptide receptors: Tools for research and therapy. *Trends Pharmacol. Sci.* **1997**, *18*, 372–386.
- (17) InsightII, a molecular modeling system, was supplied by Molecular Simulations Inc., San Diego, CA.
- (18) Stern, L. J.; Brown, J. H.; Jardetzky, T. S.; Gorga, J. C.; Urban, R. G.; Strominger, J. L.; Wiley, D. C. Crystal structure of the human class II MHC protein HLA-DR1 complexed with an influenza virus peptide. *Nature* **1994**, *368*, 215–221.
- (19) Makino, S.; Kuntz, I. D. Automated flexible ligand docking method and its application for database search. *J. Comput. Chem.* **1997**, *18*, 1812–1825.

- (20) Liu, M.; Wang, S. MCDOCK: A New Monte Carlo Docking Method for Molecular Docking Problem. *J. Comput.-Aided Mol. Design* **1999**, *13*, 435–451.
- (21) Milne, G. W. A.; Nicklaus, M. C.; Wang, S.; Driscoll, J.; Zaharevitz, D. The NCI drug information system 3D database. *J. Chem Inf. Comput. Sci.* **1994**, *34*, 1219–1224.
- (22) Voigt, J. H.; Bienfait, B.; Wang, S.; Nicklaus, M. C. Comparison of the NCI Open Database with Seven Large Chemical Structural Databases. *J. Chem. Inf. Comput. Sci.* **2001**, *41*, 702–712.
- (23) Sybyl, a molecular modeling system, was supplied by Tripos, Inc., St. Louis, MO 63144.
- (24) Tomlinson, I. P.; Bodmer, W. F. The HLA system and the analysis of multifactorial genetic disease. *Trends Genet.* **1995**, *11*, 493–498.
- (25) Smith, K. J.; Pyrdol, J.; Gauthier, L.; Wiley, D. C.; Wucherpfennig, K. Crystal structure of HLA-DR2 (DRA0101, DRB11501) complexed with a peptide from human myelin basic protein. *J. Exp. Med.* **1998**, *188*, 1511–1520.
- (26) Wucherpfennig, K. W.; Zhang, J.; Witek, C.; Matsui, M.; Modabber, Y.; Ota, K.; Hafler, D. A. Clonal expansion and persistence of human T cells specific for an immunodominant myelin basic protein peptide. *J. Immunol.* **1994**, *152*, 5581–5592.
- (27) Hurley, C. K.; Steiner, N. Differences in peptide binding of DR11 and DR13 microvariants demonstrate the power of minor variation in generating DR functional diversity. *Hum. Immunol.* **1995**, *43*, 101–112.
- (28) Rosen-Bronson, S.; Jaraquemada, D. On the relative immunogenicity of DR alloantigens: T cell recognition of HLA-DR2a and HLA-DR2b. *Hum. Immunol.* **1991**, *30*, 215–221.
- (29) Quanta, a molecular modeling system, was supplied by Accelrys, San Diego, CA.
- (30) InsightII, a molecular modeling system, was supplied by Accelrys, San Diego, CA.
- (31) Cerius², a molecular modeling system, was supplied by Accelrys Inc., San Diego, CA.
- (32) Stern, L. J.; Wiley, D. C. The human class II MHC protein HLA-DR1 assembles as empty alpha beta heterodimers in the absence of antigenic peptide. *Cell* **1992**, *68*, 465–477.
- (33) Kwok, W. W.; Nepom, G. T.; Raymond, F. D. HLA-DQ polymorphisms are highly selective for peptide binding interactions. *J. Immunol.* **1995**, *155*, 2468–2476.
- (34) Case, D. A.; Pearlman, D. A.; Caldwell, J. W.; Cheatham, T. E., III; Wang, J.; Ross, W. S.; Simmerling, C. L.; Darden, T. A.; Merz, K. M.; Stanton, R. V.; Cheng, A. L.; Vincent, J. J.; Crowley, M.; Tsui, V.; Gohlke, H.; Radmer, R. J.; Duan, Y.; Pitner, J.; Massova, I.; Seibel, G. L.; Singh, U. C.; Weiner, P. K.; Kollman, P. A. AMBER7, University of California, San Francisco, 2002.
- (35) Jorgensen, W. L.; Chandrasekhar, J.; Madura, J. D.; Impey, R. W. and Klein, M. L. Comparison of Simple Potential Functions for Simulating Liquid Water. *J. Chem. Phys.* **1983**, *79*, 926–935.
- (36) Darden, T. A.; York, D. M.; Pedersen, L. Particle Mesh Ewald—An *N*. Log(*N*) Method for Ewald Sums in Large Systems. *J. Chem. Phys.* **1993**, *98*, 10089–10092.
- (37) Enyedy, I. J.; Ling, Y.; Nacro, K.; Tomita, Y.; Wu, X.; Cao, Y.; Guo, R.; Li, B.; Zhu, X.; Huang, Y.; Long, Y.-Q.; Roller, P. P.; Yang, D.; Wang, S. Discovery of Small-Molecule Inhibitors of Bcl-2 through Structure-Based Computer Screening. *J. Med. Chem.* **2001**, *44*, 4313–4324.
- (38) SYBYL 6.9.1, a molecular modeling system, was supplied by Tripos, St. Louis, MO.
- (39) Jones, G.; Willett, P.; Glen, R. C.; Leach, A. R.; Taylor, R. Development and Validation of A Genetic Algorithm for Flexible Docking. *J. Mol. Biol.* **1997**, *267*, 727–748
- (40) Wang, R.; Lu, Y.; Wang, S. Comparative Evaluation of 11 Scoring Functions for Molecular Docking. *J. Med. Chem.* **2003**, *46*, 2287–2303.
- (41) Wallace, A. C.; Laskowski, R. A.; Thornton, J. M. LIGPLOT: A program to generate schematic diagrams of protein–ligand interactions. *Protein Eng.* **1995**, *8*, 127–134.

JM030362S